References

1   MURTZ, M., PFISTER, O., MARQUARDT, J.H., STEPHENS, M., WELLS, J.S., WALTMAN, S., HOLLBERG, L., ROBINSON, H.G., FOX, R.W., MEHUYS, D., BROWN, E.R., and MCINTOSH, K.A.: 'Nonlinear optics for optical frequency synthesis and optical divide by 3'. Proc. 5th Annual meeting of frequency standards and frequency metrology, 1995

2   LANDE, D., HEANUE, J.F., BASHAW, M.C., and HESSELINK, L.: 'A digital wavelength-multiplexed holographic data storage system', to be published in *Opt. Lett.*

3   KORN, M., KORFER, T., FORCHEL, A., and ROENTGEN, P.: 'Fabrication and optical characterisation of first-order DFB GaInP/AlGaInP laser structures at 639nm', *Electron. Lett.*, 1990, **26**, (9), pp. 614–615

4   JANG, D.-H., KANEKO, Y., and KISHINO, K.: 'Shortest wavelength (607nm) operations of GaInP/AlInP distributed Bragg reflector lasers', *Electron. Lett.*, 1992, **28**, (4), pp. 428–430

5   GAUGGEL, H.-P., GENG, C., SCHWEIZER, H., BARTH, F., HOMMEL, J., WINTERHOFF, R., and SCHOLZ, F.: 'Fabrication and operation of first-order GaInP/AlGaInP DFB lasers at room temperature', *Electron. Lett.*, 1995, **31**, (5), pp. 367–368

6   WELCH, D.F., WANG, T., and SCIFRES, D.R.: 'Low threshold current laser emitting at 637nm', *Electron. Lett.*, 1991, **27**, (9), pp. 693–694

Lasers incorporating 2D photonic bandgap mirrors

J. O'Brien, O. Painter, R. Lee, C.C. Cheng, A. Yariv and A. Scherer

Indexing terms: Semiconductor lasers, Fabry-Perot resonators

Semiconductor lasers incorporating a 2D photonic lattice as a one end mirror in a Fabry-Perot cavity are demonstrated. The photonic lattice is a 2D hexagonal close-packed array with a lattice constant of 220nm. Pulsed threshold currents of 110mA were observed from a 180μm laser.

Photonic bandgap crystals are expected to be of use in defining microcavities for modifying spontaneous emission and as highly reflective mirrors. Several reports describe the microfabrication of 1D structures [1 – 3]. Here, we describe the incorporation of a microfabricated 2D photonic lattice in an edge-emitting semiconductor laser structure. We demonstrate laser operation in a cavity formed between a cleaved facet and a microfabricated periodic lattice.

The photonic lattice used was a 2D hexagonal close-packed lattice etched vertically into the semiconductor. The lattice was designed to have a TE photonic bandgap that spectrally overlapped the gain region of the semiconductor laser structure [4]. The lattice constant a of the structure was 212nm, and the ratio of the hole diameter to the lattice constant, r/a, was ~0.33. The lattice was etched through the active region and well into the bottom waveguide cladding to ensure a good overlap with the optical field. The expected reflectivity from a smooth interface with the spatially averaged effective index of the lattice was calculated to be 2.8%.

The sample was an MBE-grown GRINSCH laser structure. The active region contained a single 10nm GaAs quantum well. The GRINSCH region was graded between $Al_{0.5}Ga_{0.5}As$ and $Al_{0.2}Ga_{0.8}As$. The doping level in the cladding was $10^{18}cm^{-3}$ for both Si and Be. A 200nm thick AlAs layer surrounded by 15nm thick $Al_{0.3}Ga_{0.7}As$ layers was included above the p-doped cladding in the top contact layers. This layer was necessary for the fabrication of the dielectric lattice as described below. The sample was capped by a 100nm thick GaAs layer that was Be doped $10^{19}cm^{-3}$.

The sample is lapped prior to processing to a thickness of 9 mils. The processing of the 2D mirrors incorporates a surface mask and an innovative AlAs MBE grown buried mask layer. Prior to depositing the multilayer surface mask, the laser top contacts were deposited along with a 300nm thick layer of sputtered Ni to protect this contact during the photonic lattice etching. The top contacts are rectangular stripes of length 254μm and width 25μm. A 15μm wide 'window' is opened between bars which

allows the 2D mirror pattern to be transferred into the semiconductor. The surface mask consists of a 60nm thick layer of SiO_2, followed by 5nm of Cr and 50nm of Au. Finally, a 70nm layer of 2% PMMA (polymethyl methacyclate) is used as electron beam resist. A hexagonal array of holes is first defined in the PMMA with a focused electron beam lithography process. Following the beam writing, the Cr/Au is milled with an Ar^+ beam (IBE). The pattern of holes is then directionally transferred through the SiO_2 with a reactive etch using C_2F_6. Subsequently, a chemically assisted ion beam etch (CAIBE) is used to transfer the holes through the 100nm GaAs cap layer and the 200nm AlAs mask layers. This results in holes that penetrate through the AlAs layer and terminate in a GaAs buffer layer. High temperature field oxidation of the AlAs is subsequently performed at 340°C for 1.5h [5]. This oxidises the AlAs around the holes and thus forms a very sturdy mask [6]. The hexagonal array of holes is then transferred to a depth of 2–3μm into the laser structure so as to overlap the optical field.

Fig. 1 shows an SEM micrograph of the etched lattice. We find that the AlO_x mask layer stands up well under CAIBE and thus holes as deep as 3μm are attainable. However, as the holes become deeper, the effects of changes in the substrate temperature result in narrowing or undercutting of the mask. To prevent thermal drift, a water cooled stage was used in the CAIBE system to etch the holes to the required depth while maintaining straight sidewalls.
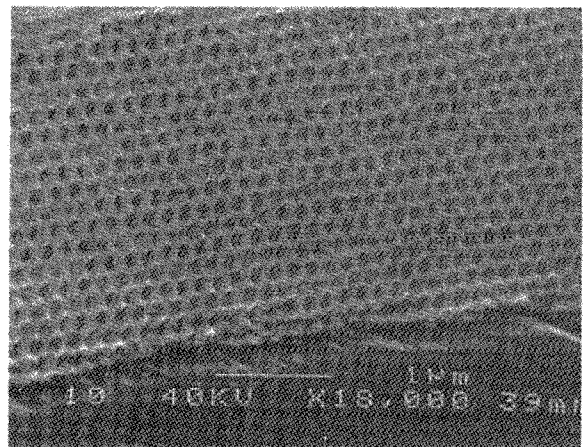

Fig. 1 *SEM micrograph of photonic lattice*

After this last CAIBE, the surface mask is gone and the Ni covered top contacts thus define a waveguide structure. In fact, owing to the slower etch rate in the holes than in the bulk semiconductor, the ridge waveguide is etched 4μm deep, right through the active region.
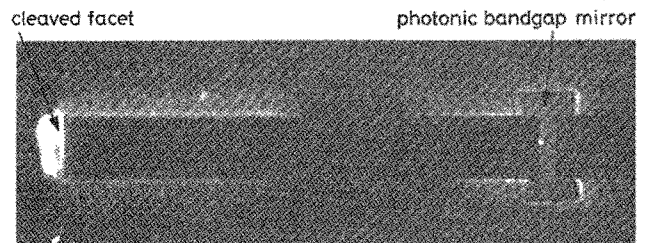

Fig. 2 *CCD camera image, taken from above, of laser above threshold*

A top view of the laser operating above threshold is shown in Fig. 2. As a final step, the back contact is deposited and the sample is cleaved up into laser bars with the longest available bar being 254μm.

The structures lased in pulsed operation. The L-I characteristic of one of these lasers is shown in Fig. 3. The light from the lasers was collected from the cleaved facets. The lowest threshold current measured was 110mA from a 180μm long laser. There was considerable scatter in the threshold currents and in the measured external efficiencies of these devices. We believe this is a result of etch depth variations and roughness in the laser stripe and in the photonic lattice. Because of this, it is very difficult to estimate a modal

mirror reflectivity for the photonic bandgap gratings. Based on the threshold current densities of the best devices, we estimate a modal reflectivity of 50% from the photonic lattice. On one sample, lasers with a dry etched facet instead of a photonic lattice were fabricated next to lasers with photonic lattices. Both lasers had cleaved facets forming the other end of the optical cavity. The emission spectrum below threshold for these two cavity types at similar bias points was measured and a Hakki-Paoli analysis indicated that the photonic lattice was eight times more reflective than the dry-etched facet. The lasers operated around 800nm which is the transition due to the second quantised state in the quantum well. One of these lasers containing a photonic grating operated in a single longitudinal mode for 80mA above threshold before becoming multimoded and eventually lasing at 850nm as well as at 800nm. The far field of these lasers, measured from the cleaved facet, had more structure than is usually observed from Fabry-Perot lasers with cleaved facets fabricated in our laboratories.
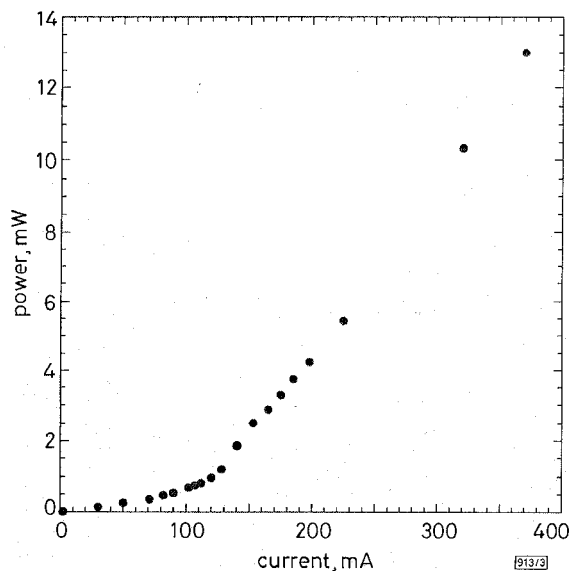

Fig. 3 *Pulsed L-I characteristic of 180 μm laser*
100ns at 30.2kHz

In summary, we have demonstrated lasers incorporating a photonic lattice as an end mirror in a Fabry-Perot cavity. The microfabricated photonic lattice consisted of a 2D hexagonal close-packed array of holes ~125nm in diameter etched 2.5μm deep into the sample. Considerable scatter was observed in the device threshold currents and external efficiencies.

J. O'Brien, O. Painter, R. Lee, C.C. Cheng, A. Yariv and A. Scherer (*California Institute of Technology, MS 128-95, Pasadena, CA 91106, USA*)

References

1 ZHANG, J.P., CHU, D.Y., WU, S.L., BI, W.G., TIBERIO, R C., JOSEPH, R.M., TAVLOVE, A., TU, C.W., and HO, S.T.: 'Nanofabrication of 1-D photonic bandgap structures along a photonic wire', *IEEE Photonics Technol. Lett.*, 1996, **8**, (4), pp. 491–493

2 BABA, T., HAMASAKI, M., WATANABE, N., KAEWPLUNG, P., MATSUTANI, A., MUKAIHARA, T., KOYAMA, F., and IGA, K.: 'A novel short-cavity laser with deep-grating distributed Bragg reflectors', *Jpn. J. Appl. Phys.*, 1996, **35**, (2B), pp. 1390–1394 (pt. 1)

3 KRAUSS, T.F., and DE LA RUE, R.: 'Optical characterization of waveguide based photonic microstructures', *Appl. Phys. Lett.*, 1996, **68**, (12), pp. 1613–1615

4 JOANNAPOULOS, J.D., MEADE, R.D., and WINN, J.N.: 'Photonic crystals' (Princeton University Press, Princeton, NJ, 1995)

5 DALLESASSE, J.M., HOLONYAK, Jr., N., SUGG, A.R., RICHARD, T.A., and EL-ZEIN, N.: 'Hydrolyzation oxidation of $Al_xGa_{1-x}As$-AlAs-GaAs quantum well heterostructures and superlattices', *Appl. Phys. Lett.*, 1990, **57**, (26), pp. 2844–2846

6 CHENG, C.C., SCHERER, A., ARBET-ENGLES, V., and YABLONOVITCH, E.: 'Lithographic bandgap tuning of 3D photonic crystals', to be published in *J. Vac. Science Technol. B*

Room-temperature continuous-wave operation of GaInNAs/GaAs laser diode

M. Kondow, S. Natatsuka, T. Kitatani, Y. Yazawa and M. Okai

A long-wavelength GaInNAs/GaAs quantum-well laser has been developed that operates under continuous-wave conditions at room temperature. Excellent high-temperature performance is demonstrated.

In current optical fibre communications, laser diodes are used in the long wavelength range to minimise transmission loss in 1.3 or 1.55μm optical fibre windows. Wide-temperature-range operation is essential in the optical access networks now being rapidly developed. Although the lasing properties of the long-wavelength InGaAsP/InP lasers are improved by using strained multiquantum layers [1], the performance at high temperature is still unsatisfactory. This is mainly because of weak electron confinement due to a low potential barrier in the conduction band. We previously proposed a novel material, GaInNAs, to drastically improve the high-temperature performance of long-wavelength lasers [2]. Using this material, a long-wavelength laser can be fabricated on a GaAs substrate and an energy discontinuity of > 300meV can be achieved in the conduction band. This should lead to a laser with a high characteristic temperature (T_0) of over 150K. Also using this material, we demonstrated the actual operation of a GaInNAs laser at 77K [3]. In this Letter, we report continuous-wave (CW) operation of a GaInNAs/GaAs single quantum-well (SQW) laser at room temperature.
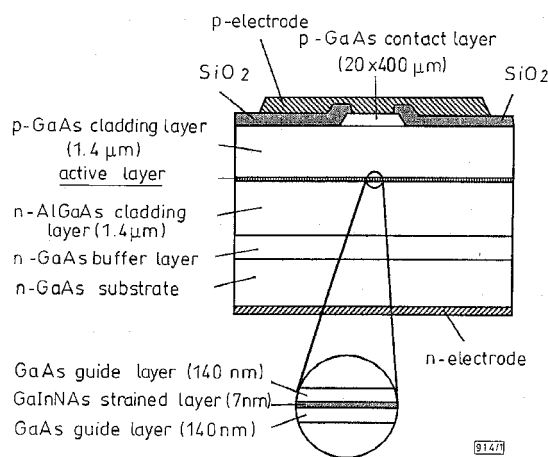

Fig. 1 *Schematic structure of GaInNAs/GaAs SQW laser*

Fig. 1 shows the schematic structure of our gain-guided type GaInNAs/GaAs SQW laser. It was grown on a (100)-oriented *n*-GaAs substrate by using gas-source molecular beam epitaxy [4]. The active layer consisted of one 7nm thick $Ga_{0.7}In_{0.3}N_{0.004}As_{0.996}$ strained layer quantum-well sandwiched between two 140nm thick GaAs unstrained guide layers. The mole fraction of the GaInNAs layer was determined by X-ray diffraction and photoluminescence measurements [4]. Since the GaInNAs layer was highly strained by ~ +2%, the critical thickness was calculated to be ~10nm. $Al_{0.3}Ga_{0.7}As$ was used for the cladding layer. The cladding layers were each 1.4 μm thick and had a carrier density of $7 \times 10^{17}cm^{-3}$.